Journal of Turbomachinery

Copy of e-mail Notification

Journal of Turbomachinery Published by ASME

Dear Author,

Congratulations on having your paper accepted for publication in the ASME Journal Program.
Your page proof is available from the ASME Proof site here:
http://cps.kwglobal.com/MIS/AuthorProofLogin.aspx?pwd=20084d7819f7&CA=AS

Login: your e-mail address
Password: 20084d7819f7

Please keep this email in case you need to refer back to it in the future.
Responsibility of detecting errors rests with the author. Please review the page proofs carefully and:

1. Answer any queries on the “Author Query Form”
2. Proofread any tables and equations carefully
3. Check to see that any special characters have translated correctly
4. Publication will not proceed until a response is received. If there are no corrections, a response is still required.

RETURNING CORRECTIONS:
Corrections must be returned using the ASME Proof Download & Corrections Submission Site (link above). You will be able to upload:

1. Annotated PDF
2. Text entry of corrections, with line numbers, in the text box provided
3. Additional files, if necessary.

SPECIAL NOTES:
Your Login and Password are valid for a limited time. Please reply within 48 hours.

Corrections not returned through the above website will be subject to publication delays.
This e-proof is to be used only for the purpose of returning corrections to the publisher.
If you have any questions, please contact: asme.cenveo@cenveo.com, and include your article no. (TURBO-17-1112) in the subject line. This email should not be used to return corrections.

Approval of these proofs re-confirms the copyright agreement provision that all necessary rights from third parties for any copyrighted material (including without limitation any diagrams, photographs, figures or text) contained in the paper has been obtained in writing and that appropriate credit has been included.

Sincerely,
Mary O'Brien, Journal Production Manager

STATEMENT OF EDITORIAL POLICY AND PRACTICE

The Technical Committee on Publications and Communications (TCPC) of ASME aims to maintain a high degree of technical, literary, and typographical excellence in its publications. Primary consideration in conducting the publications is therefore given to the interests of the reader and to safeguarding the prestige of the Society.

To this end the TCPC confidently expects that sponsor groups will subject every paper recommended by them for publication to careful and critical review for the purpose of eliminating and correcting errors and suggesting ways in which the paper may be improved as to clarity and conciseness of expression, accuracy of statement, and omission of unnecessary and irrelevant material. The primary responsibility for the technical quality of the papers rests with the sponsor groups.

In approving a paper for publication, however, the TCPC reserves the right to submit it for further review to competent critics of its own choosing if it feels that this additional precaution is desirable. The TCPC also reserves the right to request revision or condensation of a paper by the author or by the staff for approval by the author. It reserves the right, and charges the editorial staff, to eliminate or modify statements in the paper that appear to be not in good taste and hence likely to offend readers (such as obvious advertising of commercial ventures and products, comments on the intentions, character, or acts of persons and organizations that may be construed as offensive or libelous), and to suggest to authors rephrasing of sentences where this will be in the interest of clarity. Such rephrasing is kept to a minimum.

Inasmuch as specific criteria for the judging of individual cases cannot, in the opinion of the TCPC, be set up in any but the most general rules, the TCPC relies upon the editorial staff to exercise its judgment in making changes in manuscripts, in rearranging and condensing papers, and in making suggestions to authors. The TCPC realizes that the opinions of author and editor may sometimes differ, and hence it is an invariable practice that no paper is published until it has been passed on by the author. For this purpose page proofs of the edited paper are sent to the author prior to publication in a journal. Changes in content and form made in the proofs by authors are followed by the editor except in cases in which the Society's standard spelling and abbreviation forms are affected.

If important differences of opinion arise between author and editor, the points at issue are discussed in correspondence or interview, and if a solution satisfactory to both author and editor is not reached, the matter is laid before the TCPC for adjustment.

Technical Committee on Publications and Communications (TCPC)
Reviewed: 05/2012

AUTHOR QUERY FORM

ASME SETTING THE STANDARD	**Journal: J. Turbomach.** **Article Number: TURBO-17-1112**	**Please provide your responses and any corrections by annotating this PDF and uploading it to ASME's eProof website as detailed in the Welcome email.**

Dear Author,

Below are the queries associated with your article; please answer all of these queries before sending the proof back to Cenveo. Production and publication of your paper will continue after you return corrections or respond that there are no additional corrections.

Location in article	Query / Remark: click on the Q link to navigate to the appropriate spot in the proof. There, insert your comments as a PDF annotation.
AQ1	Reminder – the ASME Copyright Agreement that was signed by all authors includes the following: "You have the right to enter into this Copyright Form and to make the assignment of rights to ASME. If the Paper contains excerpts from other copyrighted material (including without limitation any diagrams, photographs, figures or text), you have acquired in writing all necessary rights from third parties to include those materials in the Paper, and have provided appropriate credit for that third-party material in footnotes or in a bibliography." As required, ASME may contact the authors to obtain a copy of the written permission.
AQ2	Any content obtained from the web and included in the paper may require written permission and appropriate credit if it is copyrighted content. If copyright status cannot be determined, this content should not be included in the paper.
AQ3	Please provide department details for affiliation. Kindly check and confirm its presentation.
AQ4	Please define "HP," "EBFOG," "HPT," "CAA," and "CFD," at first occurrence.
AQ5	Please specify which section "In the following sections" refers to here.
AQ6	Please check and confirm the hierarchy of section headings.
AQ7	Please note that general copy editing rules to set variables in italics, matrices/vectors/tensors in bold roman, chemical formulas in roman, and abbreviations in roman. So, please check and confirm the usage of bold roman across the article.
AQ8	Please specify which section "in the previous section" refers to here.
AQ9	Please specify which section "in the previous section" refers to here.
AQ10	Please provide page number in range for Ref. 1.
AQ11	Please provide page range or paper number for Ref. 6.
AQ12	Please provide issue and page number in range for Ref. 10.
AQ13	Please provide page number in range for Ref. 34.
AQ14	Please provide paper number for Ref. 19, 27, and 31.
AQ15	Please provide publisher location (city and state/country) for Ref. 23. Kindly check and confirm its presentation.
AQ16	Please provide complete publication details for Ref. 28.
AQ17	Please check and confirm the presentation of Ref. 33.
AQ18	Please provide publisher name, location (city and state/country) and accessed date for Ref. 41. Kindly check and confirm its presentation.
AQ19	Please reword caption of Fig. 6 without color words as readers of print will only see black and white figures.
AQ20	Please check and approve the edit made in the article title.
AQ21	Please check the clarity of the sentence 'The numerical analysis have been…'
AQ22	Please provide DOI or website to access article for Refs. 1 and 32.

Thank you for your assistance.

AQ1
AQ2 **Nicola Casari**[1]
■,
University of Ferrara,
Via Saragat, 1,
Ferrara (IT) 44122, Italy
e-mails: nicola.casari@unife.it;
AQ3 nicola.casari15@imperial.ac.uk

AQ20 **Michele Pinelli**
■,
University of Ferrara,
Via Saragat, 1,
Ferrara (IT) 44122, Italy

Alessio Suman
AQ4 ■,
University of Ferrara,
Via Saragat, 1,
Ferrara (IT) 44122, Italy

Luca di Mare
Osney Thermo-Fluids Laboratory,
Department of Engineering Science,
University of Oxford,
Oxford OX2 0ES,
Oxfordshire, UK

Francesco Montomoli
Imperial College London,
London SW7 2AZ, UK

EBFOG: Deposition, Erosion, and Detachment on High-Pressure Turbine Vanes

Fouling and erosion are two pressing problems that severely affect gas turbine performance and life. When aircraft fly through a volcanic ash cloud, the two phenomena occur simultaneously in the cold as well as in the hot section of the engine. In the high-pressure turbine, in particular, particles soften or melt due to the high gas temperatures and stick to the wet surfaces. The throat area, and hence the capacity, of the HP turbine is modified by these phenomena, affecting the engine stability and possibly forcing engine shutdown. This work presents a model for deposition and erosion in gas turbines and its implementation in a three-dimensional Navier–Stokes solver. Both deposition and erosion are taken into account, together with deposit detachment due to changed flow conditions. The model is based on a statistical description of the behavior of softened particles. The particles can stick to the surface or can bounce away, eroding the material. The sticking prediction relies on the authors' EBFOG model. The impinging particles which do not stick to the surface are responsible for the removal of material. The model is demonstrated on a high-pressure turbine vane. The airfoil shape evolution over the exposure time as a consequence of the impinging particles has been carefully monitored. The variation of the flow field as a consequence of the geometrical changes is reported as an important piece of on-board information for the flight crew. [DOI: 10.1115/1.4039181]

Introduction

Aircraft following normal commercial routes and flight plans can fly through dust clouds for intervals of time ranging from few seconds to several minutes [1]. During this time, a large amount of particulate is ingested by the aircraft engines. Ash clouds can carry particulate with concentrations as high as $250\,\mathrm{mg_{ash}/m^3_{air}}$ [1]. For a high thrust turbofan engine processing a mass flow rate of approximately 500 kg/s, the resulting rate of ingestion of solid contaminant can reach the order of $1\,\mathrm{kg_{ash}/s}$. The presence of particles at cruising altitude or during take-off and landing therefore poses a serious threat to the operation of aircraft engines. The seriousness of this threat is highlighted by the disruption brought to air travel by volcanic events in recent years [2].

The ingestion of particles inevitably brings about losses. Even if the size of the ingested particulate is such that the particles follow the streamlines and do not impinge against the blades, a certain amount of energy is lost due to their transport. The value of energy lost by the carrier phase in favor of the dispersed one depends on the concentration of the latter. The threshold values which cause a noticeable amount of losses are suggested, among the others, by Elghobashi [3].

The particles following the core flow are heated through the combustor. If the turbine entry temperature is sufficiently high, the particles soften and can adhere to the surrounding solid surfaces. The net particle deposition rate is determined by the likelihood of sticking and by the rate at which the main flow removes protruding deposits. In general, the deposition of particles can change the shape of the vane in an uncontrolled way. Particle sticking on the first stage nozzle of the high-pressure turbine results in an increase in aerofoil thickness and roughness. The deposits can also clog cooling holes, if present, leading to the rise of the blade surface temperature. In the most severe cases, as pointed out by Ogiriki et al. [4], this leads to a reduction in life due to thermal stresses, local overheating and creep. The increased boundary layer displacement thickness—due to the increased roughness and uncontrolled change in shape—and the build-up of the deposit can cause a reduction in passage area and hence in the turbine capacity. This, in turn, can push the compression system beyond its stability limit, making the risk of surge highly likely.

Even if the deposition does not take place, the consequences of the particle impact against a blade can cause erosion of hot section components. This leads to the permanent loss of the material and to irreversible damage. The main consequences of this problem are an increase in the clearances and in blade surface roughness and changes in the blade shape, especially in the leading and trailing edges. The outcome of this process is the permanent deterioration in turbine performance and increased repair and maintenance costs. For more detailed explanations and analysis, see, for example, Ref. [5].

The prediction of deposition and erosion rates, and of the deposit shape in the passages of high-pressure turbines is therefore a pressing and important problem. A first attempt in this track has been carried out by Casari et al. [6], but without taking into account the build-up detachment.

For what concerns the deposit modeling, two main approaches for the prediction of the sticking are currently available in the literature: the first one uses critical thresholds for particle viscosity [7] or velocity [8] above which particles stick, whereas the second method tries to represent the probability of the particle sticking. Examples of the former method are [9] and [10]. On the other hand, the latter method aims to define a sticking probability that is the likelihood a particle has to stick to a surface. This is a very common model used in the literature and an example is discussed in Ref. [11].

[1]Corresponding author.

Contributed by the International Gas Turbine Institute (IGTI) of ASME for publication in the Journal of Turbomachinery. Manuscript received August 11, 2017; final manuscript received November 2, 2017; published online xx xx, xxxx. Editor: Kenneth Hall.

The usage of the first method implies a deterministic modeling of the physics of the problem. Besides the characteristics of the particle at the impact, the particle history must be known: for instance, in the model formulated by Song et al. [10], the heating rate of the particle is a fundamental parameter for the prediction of the sticking. Seldom it is possible to obtain precisely these quantities, unless the trajectory of each particle can be simulated through the entire engine: the heating rate depends very closely on the particle trajectory through the combustor, especially if it passes through the flame. On the top of that, the chemical composition of each of the particles should be known. Indeed it is reported in the literature, for example in Ref. [12], calcium and sodium are particularly bad ingredients in the mixture because of their very low melting temperature and sticking qualities. Nonetheless, it is indeed well known that inside the same ash cloud the composition can vary in a relative wide range [13], complicating the deterministic modeling of the phenomenon. This method, even if very promising, needs further studies to be applied in a reliable manner.

In this work, the EBFOG model [14] is used to overcome the issues of the above-mentioned methods.

Another phenomenon which is likely to occur in high-pressure turbine vanes is erosion. This fact is well known and reported in the literature, for example, in Ref. [15] or [16]. In-service heavy-duty gas turbines are subject to erosion of the hot-section blades and increase in the surface roughness. These aspects are usually seen as two faces of the same coin [16]: due to particle impingement against surfaces, the rms roughness can increase of an order of magnitude [17]. The increased roughness inevitably brings about losses and increase in the boundary layer thickness. On the top of that, an enhancement of the heat transfer on the blade surface is reported in the literature [18]. One of the most used formulation for the high-pressure turbine erosion prediction is proposed by Tabakoff et al. [19] and it is the one used in this work.

Deposition of particles on the surfaces entails the build-up of material. The deposit can be detached from the surface as a consequence of the modified flow field. This phenomenon has been analyzed widely in literature and several studies on the mechanisms of detachment are available. Das et al. [20] compare the three main mechanisms of detachment, namely lifting, rolling, or sliding. The authors state that the main mechanism of detachment is the rolling of the deposited particle by breaking the interface particle-surface. There are many theories in the literature trying to find the main cause of the bond breakage. For instance, Reeks et al. [21] formulated a theory based on the transfer of turbulent energy to a particle. The particle can be resuspended from a substrate after it accumulates enough energy to escape from the adhesive potential well. Turbulent flow lift forces transfer energy by their average component, which modifies the shape and height of the well, and their random fluctuating component, which causes the particle and surface to deform in a random oscillatory fashion from their static equilibrium configurations. In this paper, the detachment is thought to be dependent only on the aerodynamic drag, and the well-known model reported in Ref. [22] is used.

In this work, a numerical study is conducted into the consequences of flying through a volcanic ash cloud. In the following AQ5 sections, the following topics will be treated:

- application of an in-house deposition model for the evaluation of a realistic deposition problem on HPT vanes;
- numerical simulation by means of a transient solver which takes into account the variation of the geometry and its effect on the fluid flow;
- simultaneous analysis of all the consequences the ingestion of a particle cloud can entail, namely erosion, deposition, and deposit detachment;
- The starting and final geometry are available in our on-line website to allow the repetition of tests and the validation of the consequences on the flow field.

Deposition and erosion are taken into account as well as the detachment of the deposited layer. The behavior of the particulate is described in terms of parcels (clusters of particles). Although the particulate ingested by the engine in case of flight through a cloud can be of very high concentration (up to 250 mg/m^3 [2]), the typical value does not exceed the threshold by which the so called one-way coupling can be safely used [3]. According to this approach, the effect the particles have on the fluid flow in terms of momentum and energy transfer is not taken into account.

In this work, the high-pressure turbine nozzle is treated as the most critical component of the whole engine in case of particles ingestion. The geometry evolution of a transonic vane subject to fouling/erosion is numerically investigated by means of a moving mesh technique which accounts for the boundary displacement. Such a kind of vane is usually more subject to fouling with respect to a subsonic one. More details regarding this remark can be found in Ref. [14].

A very last remark regards the concentration ingested by the engine. The standard for the "Safe-to-fly" conditions is provided by the CAA, as explained in Ref. [1], is equal to 2 mg/m^3. Such a threshold is a debated topic. Particles in the compression system, as reported in Ref. [12], are pulverized at the point that the average size by the time the flow reaches the environment control system (ECS) duct is lower than 10 μm. Thus, the ECS air is contaminated with foreign particles, that is the air breathed by the passengers. Such particulate size is very harmful if inhaled. Besides this several issues may arise within the control system, since the ECS air is used for the cooling of such components. It is known, see Ref. [12], that the Boeing aircraft that encounter the Mt. Redoubt eruption had to have all the aircraft electronics to be replaced before returning in operation. Furthermore, there is still a lot of uncertainty in the forecast of the cloud size and concentration. So such a threshold is for sure an important parameter but should not be addressed to with too much confidence.

Methodology

In this work, the consequences of the ingestion of a cloud on high-pressure turbine vanes are numerically investigated. The main effects of the ingestion are deposition and erosion of the surfaces exposed to the flow. The approach used in this paper is based on the method proposed by Casari et al. [14] with modifications to include the effect of erosion and detachment. The present method is outlined diagrammatically in Fig. 1 and is explained in detail below.

The flow field is first computed in absence of contaminant until convergence is achieved. At this point, particles are seeded at the inlet of the domain and for every time-step, both the carrier and the dispersed phase are updated. The particles are tracked via one-way approach and the flow field is solved through the *sonicFoam* solver with a set of given boundary conditions (see paragraph *CFD resolution of the flow field*). The deposition or erosion of the vane causes the mesh nodes on the surfaces to move. Mesh quality is maintained by solving a Laplace equation for the displacement over the computational domain. The present approach, although more time consuming than integrating the particle trajectories over a frozen flow field, gives more realistic information on the

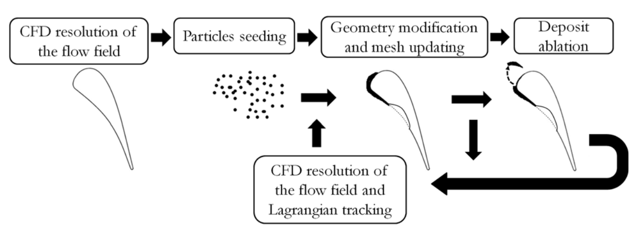

Fig. 1 Outline of the procedure, nozzle modifications not in scale

Table 1 Boundary conditions for the solver validation flow field

	Quantity	LS-89
Inlet	p_0	149,350 Pa
	T_0	420 K
	Turbulence intensity	1%
	Turbulence mixing length	0.0004 m
Wall	T	298 K
	Mis	1.02
Outlet	p	89,600 Pa

Table 2 Boundary conditions for the computation of the undisturbed flow field

	Quantity	LS-89
Inlet	p_0	1,523,000 Pa
	T_0	1708 K
	Turbulence intensity	1%
	Turbulence mixing length	0.0004 m
Wall	T	1100 K
	Mis	1.02
Outlet	p	911,200 Pa

evolution of the geometry of the vane wall. In particular, it gives the more accurate results concerning the rate of change of the passage throat area.

It must be remarked that in this work all the possible effects deriving from particles ingestion are analyzed, namely deposition, erosion, and build-up detachment. This is due to the fact that all these phenomena might happen simultaneously in the hot section of a gas turbine, as reported in Ref. [16].

AQ6 **CFD Resolution of the Flow Field.** The prediction of the deposition starts with the initialization of the flow field. In this step, no particles are transported through into domain. The numerical analysis have been carried out using the *sonicFoam* solver from AQ21 the OPENFOAM-v3.0.0 set of compressible solvers is used.

This solver is a pressure-based solver that uses the pressure implicit with splitting of operators algorithm (PISO). The solver has been validated against the well-known LS-89 test case measured by Arts et al. [23]. The boundary conditions reported in Table 1 have been applied to a 2D multiblock mesh of roughly 60,000 elements. The computational domain extends for 0.5 chord both upstream and downstream the vane. A comparison between the predicted flow field and a schlieren visualization of the flow [23] is shown in Fig. 2(*a*).

For the purpose of the ash ingestion study, a set of boundary conditions representative of cruise conditions is selected. These conditions are reported in Table 2.

In both cases, turbulence have been simulated using a k–ε model, with standard wall functions. The wall was considered to be hydraulically smooth both in cases of clean and dirty vane. It must be remarked here that this assumption is done since the deposit roughness is not known in advance. It can theoretically be either higher or lower than the original vane. To the authors' knowledge, no extensive work has been reported in literature describing the variation of the wall roughness after the deposition of volcanic ash.

Particle Seeding. Once the flow field is initialized, the injection of the particles starts at the inlet of the domain. The amount of particulate injected is derived from the following considerations.

In this work, a volcanic ash cloud with concentration of 250 mg/m^3 is considered. This concentration is representative of a very dense volcanic ash cloud [2]. A further assumption is that the same concentration that is ingested by the fan is transferred to the core flow without any changes. In such a way, the particulate flow rate that is processed by the core flow is simply a function of the by-pass ratio. This assumption is very pessimistic since a very high fraction of the foulant agent would be centrifuged toward the by-pass flow, lowering the concentration of particles within the flow processed by the turbine. Nevertheless, this condition implies more detrimental effects on the components, and so this "worst case scenario assumption" is deemed suitable for the purposes of this study. This approach is a common assumption when dealing with this kind of problem, and it is also used for the realization of the Safe-to-Fly chart by Rolls-Royce, see Ref. [1].

In this simulation, a mass flow rate of particulate equals to 1.375×10^{-7} kgs^{-1} have been injected corresponding to roughly 30,000 particles per second.

The physical properties of the particles relevant to the calculation are the density $\rho = 3000\,\mathrm{kg\ m^{-3}}$ and the specific heat $c_{\mathrm{part}} = 800$ J (kg K)$^{-1}$. The particles are inserted into the flow at the inlet of the domain at random angular positions and with velocity perfectly coupled with the fluid flow at the inlet of the domain. The size distribution is representative of the one which could reasonably reach the exit of the combustor. According to Ref. [24], the typical distribution of a volcanic ash cloud is very case dependent. Nonetheless, the biggest particles are centrifuged toward the by-pass flow or are split in smaller parts during the impact against the compressor blades. Thus, the population that approaches the high-pressure turbine vane can be represented by a uniform distribution between 1 μm and 30 μm as can be gathered

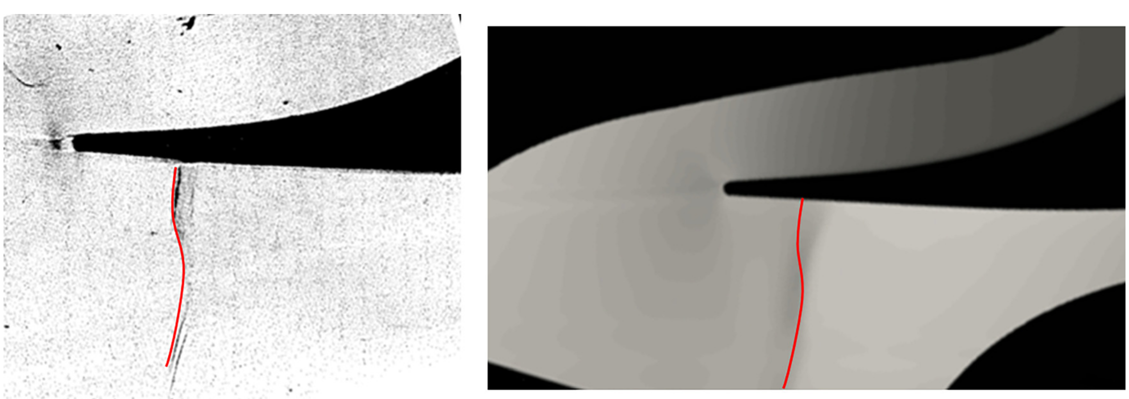

(*a*) (*b*)

Fig. 2 Schlieren visualization from Ref. [23] and results of the validating simulation: (*a*) schlieren visualization from Ref. [23] and (*b*) numerical results for validation

by Taltavull et al. [24]. The chemical composition of the particles is reported by Taltavull et al. [24]. For this composition, the coefficients for the sticking probability according to the EBFOG model are derived.

Lagrangian Tracking and Impact Modeling. Once particles are seeded, they must be tracked in order to associate the particle position with the computational cell. Since the particle concentration in the flow is small (even in the case of highly concentrated volcanic cloud), the coupling between fluid and particle is modeled through a one-way approach. The tracking algorithm provided with OPENFOAM-v3.0.0 and described in Ref. [25] is used. The motion of the particles is governed by the Basset–Boussinesq–Oseen equation, and as suggested by Rispoli et al. [26] and Wenglarz and Cohn [27], the only force to be taken into account is the drag. The balance to be solved is thus reported in the following equation:

AQ7

$$\frac{\partial \mathbf{u}_p}{\partial t} = \mathbf{F}_D = \frac{18\mu}{\rho_p d_p^2}\frac{C_D \mathrm{Re}_p}{24}(\mathbf{u}-\mathbf{u}_p) \tag{1}$$

where $\mathbf{u}$ and $\mathbf{u}_p$ are, respectively, fluid and particle velocity, $\mathbf{F}_D$ is the drag force, μ is the dynamic viscosity, ρ_p is the particle density, C_D is the drag coefficient, and Re_p is the particle Reynolds number defined as $\mathrm{Re}_p = (\rho\|\mathbf{u}-\mathbf{u}_p\|d_p)/\mu$. In this definition, d_p is the particle diameter. The default particle drag law in OPENFOAM is reported in the following equation:

$$C_D = \begin{cases} \dfrac{24}{\mathrm{Re}_p} & \text{if } \mathrm{Re}_p \le 1 \\ \dfrac{24}{\mathrm{Re}_p}\left(1+0.15\mathrm{Re}_p^{0.687}\right) & \text{if } 1 \le \mathrm{Re}_p \le 1000 \\ 0.44 & \text{if } \mathrm{Re}_p \ge 1000 \end{cases} \tag{2}$$

As one can see, the equation used for the drag is valid for spherical particles. It is well known that the shape of the volcanic ash is far from being spherical, for example, see Ref. [24]. Nonetheless, when particles pass through the combustor they melt and their shape become spherical as reported by Lau and Windand [28]. The time-step is limited by the condition that the maximum Courant–Friedrichs–Lewy number is 1. This condition is imposed for accuracy reasons related to the particle tracking [29] and guarantees that each particle crosses at most one cell boundary at every time-step.

The heat transfer between the gas and the particles is also computed. The Ranz–Marshall equation (see Eq. (3)) is used to estimate the Nusselt number for the heat transfer from the fluid to the particle

$$\mathrm{Nu} = \frac{hd_p}{k} = 2 + 0.6\sqrt{\mathrm{Re}_p}\sqrt[3]{\mathrm{Pr}} \tag{3}$$

In Eq. (3), Nu is the Nusselt number which characterizes the thermal boundary layer of the particle, h is the convection heat transfer coefficient, k is the thermal conductivity of the gas, and $\mathrm{Pr} = \mu c_p/k$ is its Prandtl Number. If Nu is known, and in this work is evaluated using the right hand side of Eq. (3), k is a property of the gas and thus h is derived. Finally $\dot{Q} = hS(T_p - T_\infty)$ can be evaluated, where T_∞ is the temperature of the gas outside the thermal boundary layer of the particle having a temperature of T_p. The variation in the particle temperature is calculated as reported in Eq. (4)

$$\frac{\partial T_p}{\partial t} = \frac{\dot{Q}}{m_p c_{\mathrm{part}}} \tag{4}$$

Impact Modeling. If a particle hits the vane, the consequences depends on the particle properties just before the impact.

Sticking. The properties of the particle at the end of the time-step before the impact are evaluated. The sticking probability is evaluated using the EBFOG model [14]. The model uses an Arrhenius-like Eq. (5) whereby the kinetic energy of the particle associated with its motion normal to the solid surface is compared with an energy which represents its state (solid, soft solid, liquid) and which depends exclusively on temperature through a law of corresponding states

$$S_p = Ae^{-\frac{C_1}{\frac{1}{2}m_p v_{p,n}^2\left(1+C_2\frac{T}{T^*}\right)}} \tag{5}$$

The reference temperature T^* is assumed to be the softening temperature of the particle material under investigation. The constant C_2 is material independent and its value is equal to 3027. From the analysis reported in Ref. [14], Eq. (4) fits the experimental data for a nonmetallic particle [24] if the coefficients are chosen to be $A = 0.897$ and $C_1 = 2.51 \times 10^{-5}$.

The outcome of the model is a number belonging to the range [0–1]. The decision whether a particle sticks or not is taken by a Metropolis–Hasting algorithm. This method uses an auxiliary random number in the range [0–1] that is compared with S_p. If the randomly generated number is greater than the coefficient provided by Eq. (5), the algorithm rejects the sticking of the particle and vice versa. In this way, the overall probability is respected and the results should reflect the actual statistics for every time-step of computation.

Erosion. If the Monte Carlo method rejects the hypothesis, the particle does not stick to the surface. It is well known that the ingestion of particle clouds entails deposition as well as erosion [30]. Thus, in this work it is assumed that a particle that does not stick to a surface brings about erosion. Therefore, in the present method, all the particles that impinge the vane either cause erosion or stick to it. To model erosion, the method proposed by Tabakoff et al. [19] is used. The ratio of the mass of eroded material to the mass of the impinging particle, ε, is predicted by Eq. (6)

$$\varepsilon = K_1\left\{1 + C_k\left[K_{12}\sin\left(\frac{90}{\beta_0}\beta_1\right)\right]\right\}^2 V_1^2\cos^2\beta_1\left[1-R_t^2\right] + K_3(V_1\sin\beta_1)^4 \tag{6}$$

For fly ash particles impinging on steel (the coefficients used in this article), $K_1 = 1.505101 \times 10^{-6}$, $K_{12} = 0.296077$, and $K_3 = 5.0 \times 10^{-12}$ (from Tabakoff et al. [19]). C_K is a parameter which value depends on β_1 (impingement angle) and β_0 (angle of maximum erosion) as follows:

$$C_k = \begin{cases} 1 & \text{if } \beta_1 \le 2\beta_0 \\ 0 & \text{if } \beta_1 > 2\beta_0 \end{cases}$$

and $R_t = 1 - V_1\sin\beta_1$. The trajectories of the particles after the rebound, if erosion takes place, are evaluated through the relations provided by Tabakoff and Malak [31]. These empirical correlations are strongly material dependent and the equations for fly ash impacting a 410 stainless steel have been implemented, as reported by Tabakoff et al. [19].

Geometry Modification and Mesh Update. Once an impact takes place, the geometry is always modified, by either loss or gain of material according to the characteristics of the impinging particle. In both cases, a displacement in the direction normal to the surface is applied. The normal-to-the-surface vector is assumed to be the vector normal to the boundary face where the impact takes place. Since the faces of the cells are flat, this assumption does not imply any interpolation error.

In order to preserve mesh quality, the displacement of the boundary is spread onto the domain in such a way that the cells that belong to a deforming patch retain an acceptable quality. The movement of the boundaries is followed by a smoothing of the displacement across the internals point. The displacement of internal nodes is determined solving a Laplace smoothing equation with constant diffusivity. It should be pointed out that the order of magnitude of the displacement due to the boundary motion for each time-step is very small (i.e., 10^{-7}), and thus the numerical grid can bear such deformation with the aid of the smoothing without problems.

Deposit Detachment. The growth of the build-up causes a reduction of the passage section, whereas the erosion widens the channel. In both cases of erosion or deposition, the effect of the changed roughness is not taken into account. The corresponding additional reduction due to increase of the displacement thickness is therefore neglected. Nevertheless, the flow field changes as a response to the changed geometry.

The evolution of the deposition and, consequently, of flow field can cause conditions around the deposit to change. In particular, if the velocity is sufficiently high, the deposit can detach from the surface and resuspend [32]. In this work, the detachment is thought to be due only to the aerodynamic drag. This is mainly responsible of the detachment according to many authors, for example, see Ref. [22]. Thus, a momentum balance is carried out in order to evaluate the drag force necessary to overcome the adhesion force. To measure the adhesion work, Soltani and Ahmadi [22] proposed a model that relates adhesion energy to the radius of the contact area between particle and surface, and the elastic properties of both wall and particle material. The drawback of this approach is that several properties of the materials under investigation must be known.

The adhesion force for ash particles on steel in the present contribution relies on the estimates by El-Batsh [33]. Once the adhesion force is known, the quantity that causes the particle detachment is the wall shear velocity. The critical value above which the deposit detachment happens is defined by the following equation:

$$u_{\tau\mathrm{critic}}^2 = \frac{CuW_A}{\rho d_p}\left(\frac{W_A}{d_p K_c}\right)^{\frac{1}{3}} \tag{7}$$

where Cu is the Cunningham correction factor, W_A is the work of adhesion, and K_c is the composite Young modulus. The critical wall shear velocity as a function of the diameter is determined using the values of the parameters in Ref. [33]. The final equation used to determine the critical shear velocity is

$$u_{\tau\mathrm{critic}} = 1.111 \times 10^{-4} h_D^{-0.871} \tag{8}$$

where h_D is the thickness of the deposit in the cell under investigation. The condition

$$u_\tau \geq u_{\tau\mathrm{critic}} \tag{9}$$

indicates that the deposit must detach from the surface. The assumption made in this work is that if the condition (9) is true, the whole build-up adhering to a boundary face is detached. This might be not completely true since a fracture can be started anywhere inside the deposit rather than at the base. No exhaustive research has been found in the literature on this topic and there seems to be no general behavior. Inspection of the work by Webb et al. [34] reveals that, depending on the material, the deposit is completely removed in the trailing edge area whereas spalling of the outer layers of the deposit is discernible in some cases. The wettability of the ash/metal interface with respect to the ash/ash interface is most likely the responsible for such a different behavior. Further work must be carried out on this topic.

Results

The method illustrated in the previous section is applied to a realistic turbine nozzle vane section in order to predict the variation in time of the vane shape due to the deposition, erosion and detachment on the surface by the particle laden flow. AQ8

Effects on Vane Shape. The simulations are started with a nominal profile and, as illustrated in the previous section, particles AQ9 are seeded at the inlet of a converged steady solution. The evolution of the deposits and of erosion patches is monitored in time. The evolution of the profile over the first second of exposure is reported in Fig. 3.

Pressure Side. It can be seen that the fouled profile after 1 s is quite different from the one after 0.1 s everywhere but around the trailing edge. Here, the profile seems to reach the asymptotic value of the displacement already in the first few steps of the simulation. This asymptotic value of the deposit thickness is

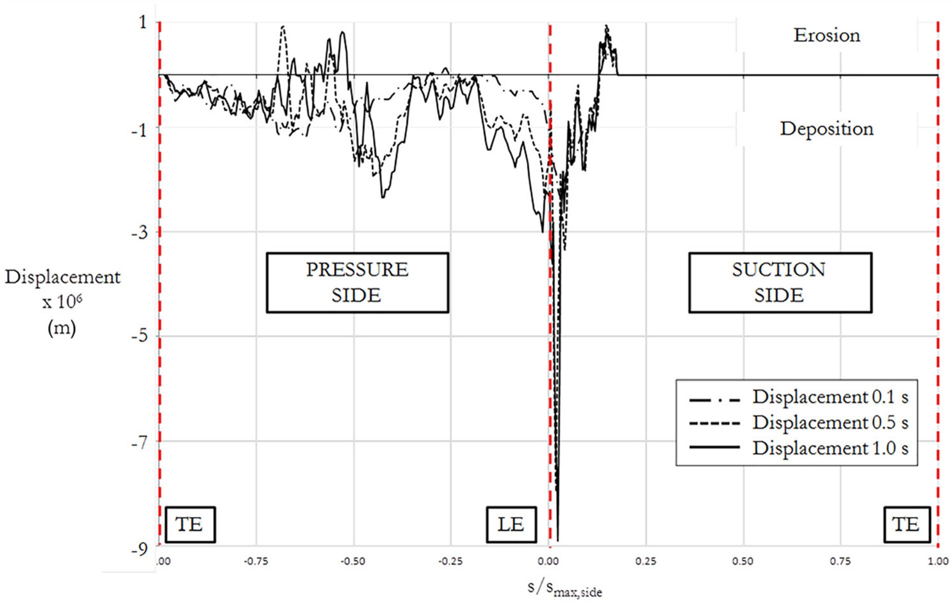

Fig. 3 Evolution of the deposit during the first second of exposure. $s_{max,side}$ stands for the maximum curvilinear coordinate on the side under investigation.

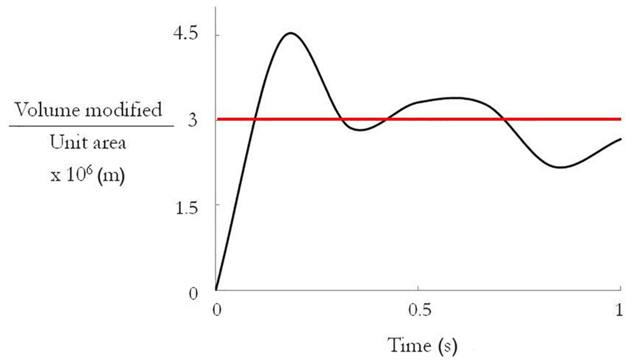

Fig. 4 Accretion of the trailing edge area

Fig. 5 Fouled geometry from Ref. [34]: particular of the thin deposit in the trailing edge area

determined by the balance between the detaching drag force and the adhesion force. The two forces act simultaneously on the deposit, and the resulting effect on the trailing edge deposit area is a continuous succession of build-up and detachment. The evolution of the trailing edge area of the pressure side is reported in Fig. 4. It can be seen that the displacement is oscillating around the asymptotic value of 3×10^{-6} m. This value remains the same for as long as the simulation had run. Unless the conditions of the deposit upstream on the vane change in such a way that the flow field is considerably modified, this value can be considered as a constant displacement. This result is in agreement with the experimental data found by Dunn [2], where very little if no deposition at all is found in the trailing edge areas.

The asymptotic value of the displacement on the trailing edge area seems to find good agreement in the experimental field. For example, the work by Webb et al. [34] reports the experimental investigation of the consequences of vane exposure to contaminated air. The study is based on a realistic vane (E^3 geometry) subject to fouling by four different types of coal ash. All the tested materials show the same behavior with respect to the trailing edge area: a thinner deposit compared with the rest of the pressure side. This feature can be considered as typical of the fouling of high-pressure turbine vanes, at least for the exposure time investigated. The appearance of a vane exposed to air contaminated with lignite is shown in Fig. 5. The circled area is considerably thinner than the other areas of the deposits.

Inspecting the other parts of the vane in Fig. 3, it can be clearly seen how the leading edge is the most affected by deposition. This remark is in good agreement with the literature (e.g., see Ref. [35,36] or [37]). Borello et al. [36] observe the same trend regarding the deposition. They do not consider the effect of erosion but, from their work, it is clear how the deposit build-up is greater on the leading edge and on the trailing edge areas, whereas no deposition occurs immediately downstream the leading edge. In this area, particle velocity components tangential to the surface are pretty high and thus the deposition is less likely. However, in Ref. [2] deposition is reported in this area of the vane for all the engine tested. We can conclude that the prevailing detrimental effect is of deposition here and it is correctly predicted in this work, even if less evident with respect to the leading edge area. Probably carrying on the simulation for longer exposure time, the difference in build-up between this area and the peak deposition at the leading edge would become lower. Other tests, for example the ones by Casaday et al. [37], show the midspan chord-wise deposition on a real turbine vane geometry. Even if the airfoil differs from the one analyzed in this work, the trend is remarkably similar to Fig. 3. The areas mentioned above are easily identifiable.

Suction Side. Parker and Lee [38] report that the highest deposition rates are found on the suction surface. This is mainly due to the small size of the particles (submicrometer). This behavior has not found agreement in the literature where real engine have been tested [2]. The other cause of deposition on the suction side is the rebound against the pressure side of the adjacent vane. In this work, no deposit on the suction surface is reported since the particle size is well above the submicrometer size. On the other hand, the rebound on the pressure surface do not cause the particle trajectory to impinge the next suction surface. For the diameters under investigation in this work, the Stokes number is such that the particle is not able to reach that surface and is brought downstream by the core flow. From Fig. 3, the suction side is affected only in proximity of the leading edge. Moving along the suction surface from the leading toward the trailing edge, an area of high deposition rate is found. Immediately downstream this area of erosion is found. This area is clearly identifiable from the beginning of the computation, and the amount of erosion seems to reach an asymptote after 1 s. It must be remarked that the entity of erosion is very little if compared with the mean deposit build-up. On the top of that, having reach an asymptote, its value is likely to remain the same and to be always less important in terms of effects on the flow field. This result is in agreement with the experiments carried out in Ref. [2], where very little erosion has been found. Beyond $s/s_{\mathrm{max,side}} = 0.25$, no changes in shape are reported in the range of time investigated.

Effects on the Flow Field. The flow field is affected by the presence of the deposit. In agreement with the results reported in Ref. [39], the shock wave is shifted downstream. Figures 6(*b*) and 7 report this shift. The isentropic Mach distribution along the suction side of the vane at the beginning and after 1 s of exposure is shown in Fig. 7.

The pressure side is not shown since the difference in the pressure distribution before and after the exposure is not noticeable. It is well clear that the overall performances of the vane is not affected except at the trailing edge. The discontinuous pressure rise (and consequent drop in the isentropic Mach number) due to the shock wave also moves streamwise.

Another parameter of paramount importance for the vane performance is the total pressure loss. As it is well known, the parameter which is usually referred to when dealing with losses is the coefficient of pressure, $c_p = (p_{02} - p_{01})/(0.5\rho_2 U_2^2)$ where the subscript 1 refers to the inlet of the computational domain and 2 to the outlet as suggested by El-Batsh [33]. U_2 is evaluated from the isentropic exit Mach number. In Fig. 8, the trend of c_p along a pitch is reported. After the exposure, the c_p is lower and this is probably due to the displacement of the shock structures. The Mach number discontinuity across the shock is therefore different and thus a variation in the c_p is the consequence. Furthermore, the wake is slightly displaced: the exit flow angle varies with the build-up of deposits on the vane surface. No reports regarding this effect on turbines have been found in the literature so far. Gbadebo et al. [40] reports the effects of artificially added roughness to compressor vanes on several parameters. The authors identify the location which affects the flow deviation the most: enlarged

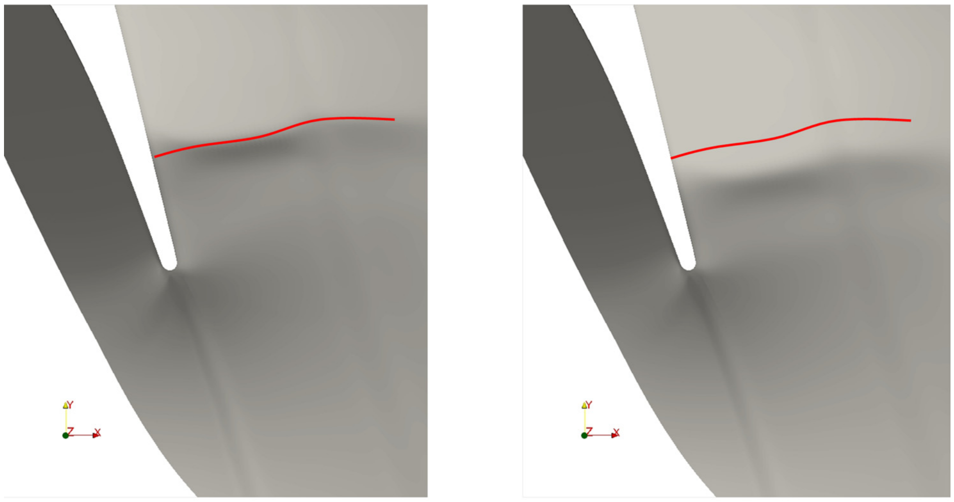

AQ19

Fig. 6 Displacement of the shock wave: depicted in red the initial position: (*a*) original position of the shock and (*b*) displacement of the shock after 1 s of exposure

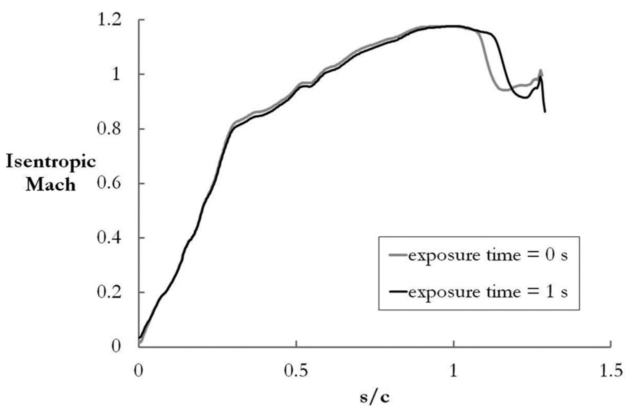

Fig. 7 Isentropic Mach distribution along the suction side of the vane at different exposure time

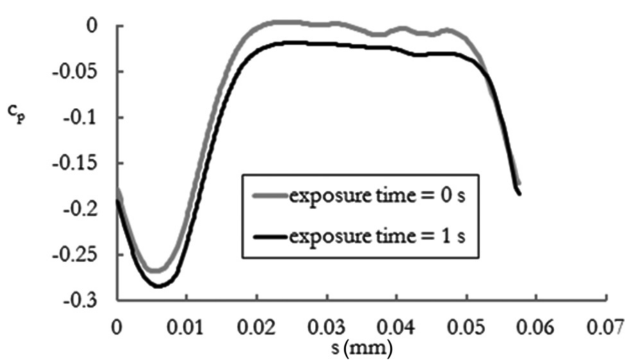

Fig. 8 Coefficient of pressure in the two cases: peak represents the wake

roughness at the leading edge seems to have the biggest effect on the outflow angle. In this work, in the leading edge area there is the biggest deposition, as reported in Fig. 3 and it is reasonable to expect a slight variation in the outflow angle. Figure 8 seems to confirm this trend. It must be remarked that the reason of the variation of the outflow angle could be also the downstream displacement of the shock.

Conclusions

The effects of the ingestion of an ash cloud have been numerically investigated. The model used is an extension of the energy-based EBFOG model which implementation has been changed in order to keep into account also the erosion. The variation of the blade shape due to erosion and sticking is accounted for by modifying the computational mesh. The build-up of the deposit can vary during time as a consequence of the aerodynamic drag. Drag force tends to detach the deposit especially in the trailing edge area where the wall shear stress and thus the friction velocity are higher. The assumption of the total detach of the local deposit rather than outer layer spallation is justified by the presence of an interface metal/nonmetal, where the chemical bonds are reasonably weaker.

Some interesting facts about the variation of the blade shape have been found. Particularly two asymptotic values can be detected, one in the peak-valley displacement in the leading-edge suction side area and the other one in the trailing-edge deposit. The asymptotic thickness is a function of the material (since the adhesion force depends on the materials that constitute the two part of the interface). In both the cases after 0.1 s of exposure, the erosion/deposition pattern on this area is remarkably similar to the one at 1 s.

On the top of that, it has been found that geometrical variations and the flow field are strictly coupled. In particular, the shock location changes due to the geometrical variations.

From this work, it can be concluded that during the ingestion of a volcanic ash cloud, the geometry of the high-pressure turbine vane changes and these variations affect the flow field in different ways. The displacement of the shock structures and a variation in the coefficient of pressure are the two main consequences.

Future work will be focused on the translation of information obtained from this article to important piece of on-board information for the flight crew. In order to predict the displacement of the operating point on the compressor map, the whole 3D vane should be investigated. Nonetheless, useful information can be derived from the fouled geometry reported in the Appendix and particularly in Fig. 9. For more quantitative analyses, the coordinates of the clean and fouled blade are available for downloading at the website [41].

Nomenclature

A = pre-exponential constant

c_p = coefficient of pressure

c_{part} = particle specific heat
C_D = drag coefficient
C_1 = activation energy—constant part
C_2 = universal constant of the reduced temperature
Cu = Cunningham correction factor
d_p = particle diameter
E_{act} = activation energy
E_{case} = reference energy for the case
h = convection heat transfer coefficient
h_D = deposit thickness
k = thermal conductivity
K_C = composite Young modulus
m_p = particle mass
Nu = Nusselt number
p = pressure
Pr = Prandtl number
$\dot{Q}$ = heat transfer per unit time
S = particle surface
S_p = sticking probability
T = temperature
T_p = particle temperature
T^* = reference temperature
U = fluid velocity
u_p = particle velocity component
u_τ = friction velocity
$u_{\tau\text{critic}}$ = critical friction velocity
V_1 = particle velocity component before impact
V_2 = particle velocity component after impact

Greek Symbols

β = impingement angle
μ = fluid viscosity
ρ = gas density
ρ_p = particle density

Appendix: Initial and Final Blade Geometry

The coordinates are available at [41].

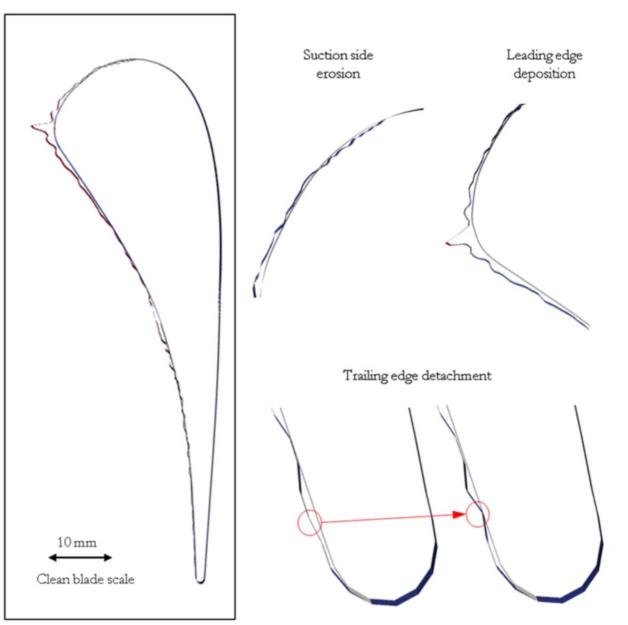

Fig. 9 Overall of the blade and details of leading edge, suction side, and trailing edge. Displacement is magnificated of 200 times.

References

[1] Clarkson, R. J., Majewicz, E. J., and Mack, P., 2016, "A Re-Evaluation of the 2010 Quantitative Understanding of the Effects Volcanic Ash Has on Gas Turbine Engines," Proc. Inst. Mech. Eng., Part G, **230**(12), ■. AQ22 AQ10

[2] Dunn, M. G., 2012, "Operation of Gas Turbine Engines in an Environment Contaminated With Volcanic Ash," ASME J. Turbomach., **134**(5), p. 051001.

[3] Elghobashi, S., 1994, "On Predicting Particle-Laden Turbulent Flows," Appl. Sci. Res., **52**(4), pp. 309–329.

[4] Ogiriki, E. A., Li, Y. G., Nikolaidis, T., Isaiah, T. E., and Sule, G., 2015, "Effect of Fouling, Thermal Barrier Coating Degradation and Film Cooling Holes Blockage on Gas Turbine Engine Creep Life," Procedia CIRP, **38**, pp. 228–233.

[5] Hamed, A., and Kuhn, T. P., 1995, "Effects of Variational Particle Restitution Characteristics on Turbomachinery Erosion," ASME J. Eng. Gas Turbines Power, **117**(3), pp. 432–440.

[6] Casari, N., Pinelli, M., Suman, A., Di Mare, L., and Montomoli, F., 2017, "Gas Turbine Blade Geometry Variation Due to Fouling," 12th European Conference on Turbomachinery Fluid Dynamics and Thermodynamics (ETC 2017), ■. AQ11

[7] Walsh, P., Sayre, A., Loehden, D., Monroe, L., Beér, J., and Sarofim, A., 1990, "Deposition of Bituminous Coal Ash on an Isolated Heat Exchanger Tube: Effects of Coal Properties on Deposit Growth," Prog. Energy Combust. Sci., **16**(4), pp. 327–345.

[8] Brach, R. M., and Dunn, P. F., 1992, "A Mathematical Model of the Impact and Adhesion of Microspheres," Aerosol Sci. Technol., **16**(1), pp. 51–64.

[9] Kleinhans, U., Wieland, C., Babat, S., Scheffknecht, G., and Spliethoff, H., 2016, "Ash Particle Sticking and Rebound Behavior: A Mechanistic Explanation and Modeling Approach," Proc. Combust. Inst., **36**(2), pp. 2341–2350.

[10] Song, W., Lavallée, Y., Hess, K.-U., Kueppers, U., Cimarelli, C., and Dingwell, D. B., 2016, "Volcanic Ash Melting Under Conditions Relevant to Ash Turbine Interactions," Nat. Commun., **7**, ■. AQ12

[11] Singh, S., and Tafti, D., 2015, "Particle Deposition Model for Particulate Flows at High Temperatures in Gas Turbine Components," Int. J. Heat Fluid Flow, **52**, pp. 72–83.

[12] Cosher, C. R., and Dunn, M. G., 2016, "Comparison of the Sensitivity to Foreign Particle Ingestion of the Ge-F101 and P/W-F100 Engines to Modern Aircraft Engines," ASME J. Eng. Gas Turbines Power, **138**(12), p. 121201.

[13] Taylor, H., and Lichte, F., 1980, "Chemical Composition of Mount St. Helens Volcanic Ash," Geophys. Res. Lett., **7**(11), pp. 949–952. AQ13

[14] Casari, N., Pinelli, M., Suman, A., di Mare, L., and Montomoli, F., 2017, "An Energy-Based Fouling Model for Gas Turbines: EBFOG," ASME J. Turbomach., **139**(2), p. 021002.

[15] Hamed, A., Tabakoff, W., Rivir, R., Das, K., and Arora, P., 2005, "Turbine Blade Surface Deterioration by Erosion," ASME J. Turbomach., **127**(3), pp. 445–452.

[16] Bons, J., Taylor, R., McClain, S., and Rivir, R., 2001, "The Many Faces of Turbine Surface Roughness," ASME J. Turbomach., **123**(4), pp. 739–748.

[17] Taylor, R., 1990, "Surface Roughness Measurements on Gas Turbine Blades," ASME J. Turbomach., **112**(2), pp. 175–180.

[18] Tarada, F., and Suzuki, M., 1993, "External Heat Transfer Enhancement to Turbine Blading Due to Surface Roughness," ASME Paper No. 93-GT-074.

[19] Tabakoff, W., Hamed, A., and Metwally, M., 1990, "Effect of Particle Size Distribution on Particle Dynamics and Blade Erosion in Axial Flow Turbines," ASME Paper No. ■. AQ14

[20] Das, S. K., Sharma, M. M., and Schechter, R. S., 1995, "Adhesion and Hydrodynamic Removal of Colloidal Particles From Surfaces," Part. Sci. Technol., **13**(3–4), pp. 227–247.

[21] Reeks, M., Reed, J., and Hall, D., 1988, "On the Resuspension of Small Particles by a Turbulent Flow," J. Phys. D: Appl. Phys., **21**(4), p. 574.

[22] Soltani, M., and Ahmadi, G., 1994, "On Particle Adhesion and Removal Mechanisms in Turbulent Flows," J. Adhes. Sci. Technol., **8**(7), pp. 763–785.

[23] Arts, T., Lambertderouvroit, M., and Rutherford, A., 1990, "Aero-Thermal Investigation of a Highly Loaded Transonic Linear Turbine Guide Vane Cascade: A Test Case for Inviscid and Viscous Flow Computations," NASA STI/Recon, ■, Technical Report No. 91. AQ15

[24] Taltavull, C., Dean, J., and Clyne, T. W., 2016, "Adhesion of Volcanic Ash Particles Under Controlled Conditions and Implications for Their Deposition in Gas Turbines," Adv. Eng. Mater., **18**(5), pp. 803–813.

[25] Macpherson, G. B., Nordin, N., and Weller, H. G., 2009, "Particle Tracking in Unstructured, Arbitrary Polyhedral Meshes for Use in CFD and Molecular Dynamics," Commun. Numer. Methods Eng., **25**(3), pp. 263–273.

[26] Rispoli, F., Delibra, G., Venturini, P., Corsini, A., Saavedra, R., and Tezduyar, T. E., 2015, "Particle Tracking and Particle–Shock Interaction in Compressible-Flow Computations With the V-SGS Stabilization and $YZ\beta$ Shock-Capturing," Comput. Mech., **55**(6), pp. 1201–1209.

[27] Wenglarz, R., and Cohn, A., 1983, "Turbine Deposition Evaluations Using Simplified Tests," ASME Paper No. ■.

[28] Lau, H., and Windand, M., 2014, "Thermal Protection Layer Destroyed, Sensors Blocked," ■. AQ16

[29] López, A., Nicholls, W., Stickland, M. T., and Dempster, W. M., 2015, "CFD Study of Jet Impingement Test Erosion Using Ansys Fluent® and OpenFoam®," Comput. Phys. Commun., **197**, pp. 88–95.

[30] Grant, G., and Tabakoff, W., 1975, "Erosion Prediction in Turbomachinery Resulting From Environmental Solid Particles," J. Aircr., **12**(5), pp. 471–478.

[31] Tabakoff, W., and Malak, M. F., 1985, "Laser Measurements of Fly Ash Rebound Parameters for Use in Trajectory Calculations," ASME Paper No. ■.

[32] Tippayawong, N., and Preechawuttipong, I., 2011, "Analytical Prediction of Particle Detachment From a Flat Surface by Turbulent Air Flows," Chiang Mai J. Sci., **38**(3), pp. 503–507.

AQ17 [33] El-Batsh, M. H., 2001, "Modeling Particle Deposition on Compressor and Turbine Blade Surfaces," Ph.D. thesis, Vienna University of Technology, Vienna, Austria.

[34] Webb, J., Casaday, B., Barker, B., Bons, J., Gledhill, A., and Padture, N., 2012, "Coal Ash Deposition on Nozzle Guide Vanes—Part I: Experimental Characteristics of Four Coal Ash Types," ASME J. Turbomach., **135**(2), p. 021033.

[35] Prenter, R., Ameri, A., and Bons, J. P., 2016, "Deposition on a Cooled Nozzle Guide Vane With Nonuniform Inlet Temperatures," ASME J. Turbomach., **138**(10), p. 101005.

[36] Borello, D., D'Angeli, L., Salvagni, A., Venturini, P., and Rispoli, F., 2014, "Study of Particles Deposition in Gas Turbine Blades in Presence of Film Cooling," ASME Paper No. GT2014-26250.

[37] Casaday, B., Prenter, R., Bonilla, C., Lawrence, M., Clum, C., Ameri, A. A., and Bons, J. P., 2014, "Deposition With Hot Streaks in an Uncooled Turbine Vane Passage," ASME J. Turbomach., **136**(4), p. 041017.

[38] Parker, G., and Lee, P., 1972, "Studies of the Deposition of Sub-Micron Particles on Turbine Blades," Proc. Inst. Mech. Eng., **186**(1), pp. 519–526.

[39] Bölcs, A., and Sari, O., 1988, "Influence of Deposit on the Flow in a Turbine Cascade," ASME J. Turbomach., **110**(4), pp. 512–519.

[40] Gbadebo, S. A., Hynes, T. P., and Cumpsty, N. A., 2004, "Influence of Surface Roughness on Three-Dimensional Separation in Axial Compressors," ASME Paper No. GT2004-53619.

[41] Casari, N., Pinelli, M., Suman, A., Di Mare, L., and Montomoli, F., 2017, "UQ Lab - EBFOG Deposition Data," ■, ■, ■, http://wwwf.imperial.ac.uk/aeronautics/research/montomolilab/nicola.html AQ18